June 2009

Analysis of MIG-10 interactors

Jessica Sullivan-Keizer
Worcester Polytechnic Institute

Project Number: EFR-0902

Analysis of *mig-10* interactors

A Major Qualifying Project Report:
Submitted to the Faculty
of the
WORCESTER POLYTECHNIC INSTITUTE
in partial fulfillment of the requirements for the
Degree of Bachelor of Science
by

Jessica Sullivan-Keizer

Date: April 27, 2009

Approved:

Prof. Elizabeth Ryder, Major Advisor

Abstract

The MIG-10 protein has been shown to be involved in cell migration and axon guidance in *C. elegans*; however, the exact mechanism is still unknown. Previous studies suggest several proteins may interact with MIG-10, including ABI-1, LIN-53, and UNC-53. To further investigate the function of these proteins, viable mutant strains were created and effects on cell migration and process guidance were assessed *in vivo*. Results suggest that ABI-1, a component of the actin polymerization machinery, and LIN-53, a nucleosome remodeling factor, both have an effect on neuronal cell migration.

Acknowledgments

I would like to thank my advisor Professor Elizabeth Ryder for her constant aid and support while completing the project. I would also like to thank Samual Politz, Michelle Debuke and Christina Grant for their help to the project as well as the Stringham lab for supplying strains.

Table of Contents

Table of Figures

Table of Tables

Introduction

Cell migration and axon guidance in nervous system development

Early steps in neuronal development, such as axon guidance, are essential in establishing the neural connectivity in a normal nervous system. During axon guidance the extension of the growth cone, at the tip of the extending axon, is directed by specific guidance cues. These guidance cues include slits, netrins, ephrins and semaphorins (Quinn and Wadsworth, 2008). F-actin and microtubules accumulate in the growth cone in response to the guidance molecules, causing axon growth in the direction of accumulation.

Cell migration has a similar mechanism as axon guidance. The cell polarizes into a 'front,' forward moving, and 'back,' rear retracting, portion in response to external promoting cues. After encountering these promoting molecules, the cell undergoes cycles of cell front extension and back retraction (Vicente-Manzanares, Webb & Horwitz, 2005). Front extension is heavily dependent on the creation of actin filaments and so the entire process is affected by actin polymerization and its related proteins. Though much research has been done on axon guidance and cell migration, the signaling pathways connecting cell surface receptors to changes in actin polymerization are not fully understood.

MRL adaptor proteins, MIG-10 and its homologs RIAM and lamellopodin, have been shown to determine the direction of axon growth by mediating the localization of actin polymerization (Chang et al., 2006; Lafuente et al, 2004; Quinn et al., 2006; Quinn and Wadsworth, 2008). MIG-10 has also been shown to directly respond to the presence of guidance cues through enhanced directional growth in the presence of UNC-6/Netrin or SLT-1/Slit and misguided processes in the absence of adequate guidance cues (Quinn and Wadsworth, 2008). Further research into MIG-10 and its molecular partners in *C. elegans* will provide valuable insight into neuronal migration and related pathways in humans.

C. elegans as a Model Organism

Caenorhabditis elegans (*C. elegans*) has become an invaluable model organism in studying development, neurobiology and other biological functions since its introduction in 1974 (Brenner, 1974). The small eukaryotic nematode is an invaluable model for many reasons including its fast life cycle, easy manipulation in the laboratory and relatively small genome, 9.7 x 10^7 base pairs, which has been completely sequenced. Due to wild type invariability and the extent to which *C. elegans* have been used to study development, the cell developmental patterns have been characterized in depth (Manser and Wood, 1990). *C. elegans* is ideal for studying the nervous system as the animals have a much simpler system than more complex organisms, having only 302 neurons, while conserving neuron structure and function. Despite the differences there are many genes in *C.elegans* which have orthologs in *Homo sapiens*. Due to these orthologs, the study of gene function in *C.* elegans is relevant to similar processes in humans.

MIG-10

MIG-10 is essential to cell migration during development in *C. elegans*. It is required for the embryonic migration of the Canal Associated Neuron (CAN), Anterior Lateral Microtubule cell (ALM) and Hermaphrodite Specific Neuron (HSN), along with the extension of the posterior excretory canal (Manser and Wood, 1990). Similarly to the neural cells in the nervous system, the excretory canal must undergo migration during normal development in order to form a functioning excretory system. The excretory cell extends four canals which form junctions with the other cells of the excretory system as well as conduct outflow created during osmoregulation and metabolite reduction (wormatlas). During embryogenesis and L1, the long process (canal) of the excretory cell migrates the length of the animal. (Figure 1) In MIG-10 mutants the CAN, ALM and HSN cells migrate incompletely and the excretory canal is not fully developed. MIG-10 is most likely located downstream of UNC-6/Netrin and SLT-1/slt and acts with UNC-34. Unc-34 encodes a *C.elegans* Ena/VASP homolog which probably functions downstream of UNC-6/Netrin and SLT-1/Slt to regulate actin polymerization. UNC-34 also binds the MRL proteins *in vitro*, which suggests that it may be a link between guidance cues and axon outgrowth. (wormbase)

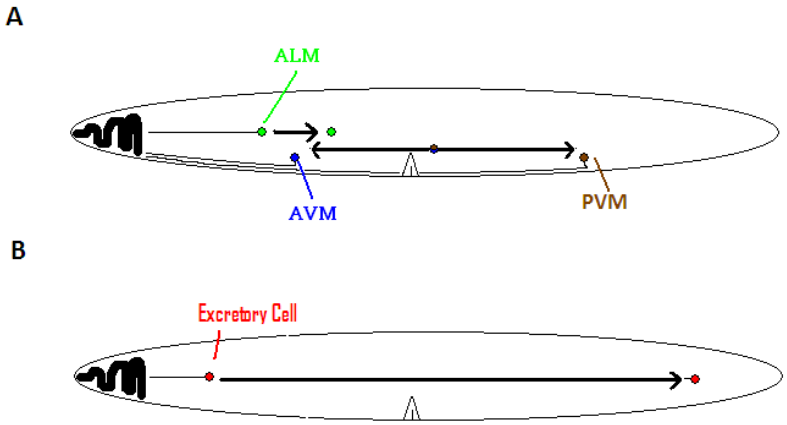

Figure 1: Migrations of mechanosensory neurons and the excretory canal in wild type *C. elegans* A) Neural cell positions. The ALM migrates anterior to posterior during embryogenesis. AVM migrates posterior to anterior during L1. AVM and PVM are actually descendents of cells that migrate. B) Excretory Cell migration. The excretory canal migrates posteriorly from an initial position near the pharynx.

MIG-10 belong to the MRL family of adaptor proteins and is homologous to the vertebrate RIAM and lamellopodin which are related to the GRB7, 10 and 14 cytoplasmic adaptor proteins (Lafuente et al, 2004; Manser and Wood, 1990; Manser et al, 1997; wormbase). The MRL proteins have a conserved domain structure with a Ras-association (RA) and pleckstrin-homology (PH) domains as well as flanking proline-rich (PR) domains. (Figure 2)

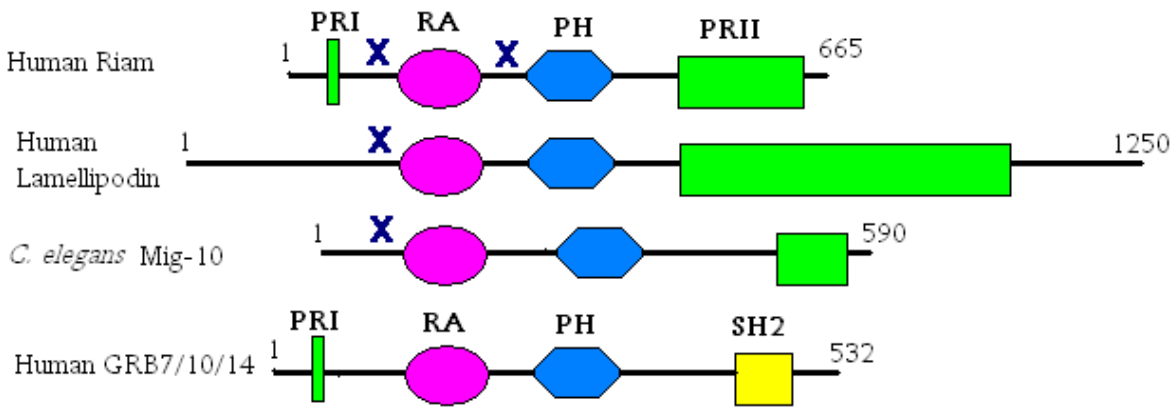

Figure 2: MRL protein family (Lafuente et al, 2004; Legg and Machesky, 2004). The MRL family of proteins and the related GRB 7, 10 and 14 share conserved domains. PH – pleckstrin homology domain; PRI/PRII – Proline Rich domain; RA – Ras association domain; SH2 – src-homology-2 domain; Blue cross – putative coiled-coil domain.

A model for MIG-10 function has been proposed in which the axon growth cone encounters extracellular guidance cues, such as UNC-6/Netrin and SLT-1/slits, and promotes Ras and PI3 kinase protein activation. The MIG-10 protein localizes to the cell membrane and associates with the Ras-related proteins and PIP2 via its RA and PH domain. The MIG-10 protein's PR domain interacts with the EVH1 domain of the Ena/VASP protein UNC-34, allowing for its localization. In response to the activation of UNC-34, actin polymerization begins (Chang et al, 2006; Quinn et al, 2006). (Figure 3)

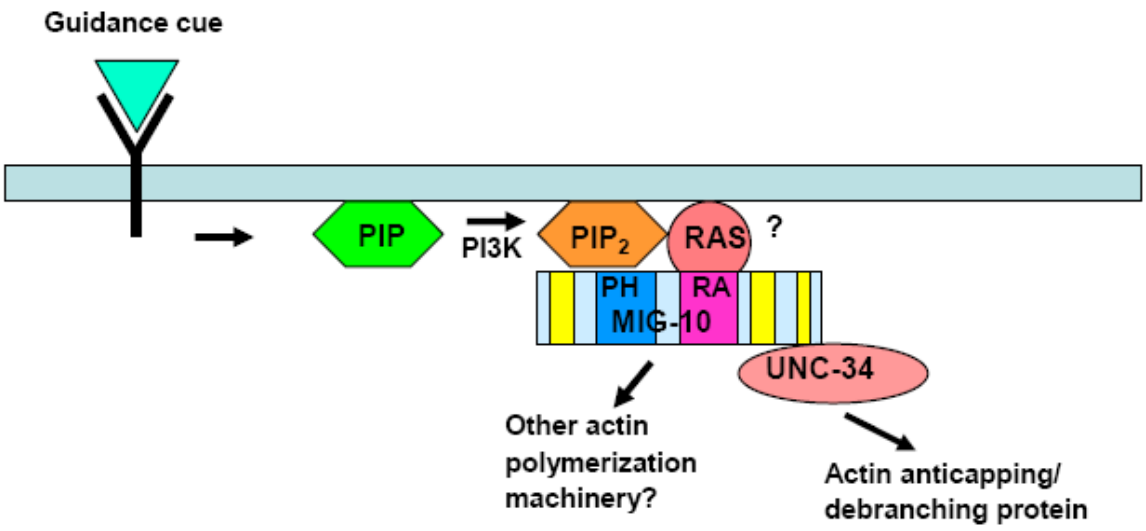

Figure 3: Speculative model for MIG-10 signal cascade (Fioccociello and Ryder, 2007). A PI3 kinase and Ras family GTPase are recruited and activated via extracellular guidance cues. The kinase substrate (PIP_2) and GTPase (Ras) localize MIG-10 and the actin polymerization machinery. PIP_2 is recognized by MIG-10's PH domain. PIP (phosphatidyl inositol); PH – pleckstrin homology domain; RA – Ras association domain; Ras – monomeric GTPase; UNC-34 – ENA/VASP protein.

Other candidates for proteins in the MIG-10 pathway

In a previous WPI Major Qualifying Project, a yeast two hybrid screen was performed to identify possible MIG-10 interactors. The study found that LIN-53 and ABI-1 were both candidates for interacting with MIG-10 (O'Toole and Gosselin, 2008).

abi-1 encodes a protein which is involved in the actin polymerization machinery and has been shown to directly cooperate with another protein identified in the yeast two hybrid screen, ARX-3 (Disanza et al, 2005;O'Toole and Gosselin, 2008). *abi-1* mutants have been shown to have abnormal excretory canal migration and motoneuron axon defects (Schmidt et al, 2009). Interaction of ABI-1 and MIG-10 would support the proposed model of MIG-10 function in which actin polymerizing proteins are most likely recruited in axon guidance by guidance cues. (O'Toole and Gosselin, 2008)

Unc-53 mutants have a phenotype similar to both *mig-10* and *abi-1* mutants in excretory canal as well as mechanosensory and motoneuron axon migration. (Schmidt et al, 2009). UNC-53 has not only been shown to interact with ABI-1, but also appears to be required for longitudinal migration of nervous tracts (Hekimi and Kershaw, 1993) and the final course of the excretory canals from the mid-body region to the tail of the animal, suggesting that it is involved in the anteroposterior (AP) guidance system (Stringham et al, 2002). Mutant phenotypes include early termination of axonal migration in lateral microtubule cells, ie. ALM and PLM, and excretory canals as well as defects in vulva development (Stringham et al., 2002).

lin-53 encodes a protein similar to RB binding protein RbAp48 which is associated with chromatin remodeling. LIN-53, which is a nucleosome remodeling factor, has been shown to work in opposition to the Ras signaling pathway (Xiaowei and Horvitz, 1998). It has also been shown to be involved in embryonic and vulva development; *lin-53* mutations result in a multi vulva phenotype (wormbase). LIN-53 could be involved in a signal cascade, in which an interaction with MIG-10 could influence gene expression (O'Toole and Gosselin, 2008).

Goals

The goal of this Major Qualifying Project (MQP) was to follow up the findings of a previous MQP (O'Toole and Gosselin, 2008) and confirm the MIG-10 interactors found during a yeast two hybrid screen are relevant *in vivo*. The goal of this project can be divided into two steps: To create viable mutant strains of the MIG-10 interactors labeled with markers of the excretory canal or migratory neurons and then to assess the effects of the mutations on cell migration and excretory canal outgrowth *in vivo*. *Abi-1*, *lin-53* and *unc-53* were chosen to be studied during this project. Assessing the phenotypes of the mutants allowed further refinement of the model for MIG-10 function.

Materials and Methods

Maintaining Strains

Both stock and created strains were maintained throughout the duration of the project. *C. elegans* strains were grown on Nematode Growth Medium (NGM) agar plates spotted with *E.coli.* The strains found in Table 1 are the strains, both stock and created, which were maintained.

Strain Name	Info	Created from	Source
RY0900	him-5(e1490);bg1s312::GFP		Prof. Ryder
RY0901	him-5(e1490);pgp12::GFP	him-5(e1490);flp20::GFP sIs10089	created
RY0902	him-5(e1490);flp20::GFP	him-5(e1490);bg1s312::GFP flp-20::GFP	created
FX494	abi-1(tm494)		Mitani lab
VA74	abi-1(tm494);pgp-12::GFP		Stringham lab
RY0200	abi-1;flp-20::GFP	mIn1(dpy:GFP)/unc-53; pgp-12:GFP him-5;flp-20::GFP abi-1;pgp-12::GFP	created
MT8840	dpy-5(e61) lin-53 (n833)		CGC
MT10408	lin-53(n833);unc76(e911); lin15A		CGC
			CGC(?)
RY0903	dpy-5(e61) lin-53(n833);pgp-12::GFP	MT8840 him-5;pgp-12::GFP	created
RY0904	dpy-5(e61) lin-53(n833);flp-20::GFP	MT8840 him-5;flp-20::GFP	created
JK2739	lin-6(e1466) dpy-5(e61) I/hT2[bli-4(e937) let-?(q782) qIs48] (I;III)		CGC
	mIn1 (dpy)/unc53(n152); pgp-12::GFP		Stringham lab
	unc-53(n166)		Stringham lab
RY0905	unc-53(n166);pgp-12::GFP	mIn(dpy)/unc53;pgp-12::GFP	Created
RY0906	unc-53(n166);flp-20::GFP	unc-53(?);pgp-12::GFP him-5;flp-20::GFP	created
BW315	mig-10(ct41)		CGC
RY0907	mig-10;flp-20::GFP		Prof. Ryder
RY0908	mig-10;pgp-12::GFP	mig-10;flp-20::GFP him-5;pgp-12::GFP	Created
RY0108	mig-10;bg1s312::GFP		Prof. Ryder

Table 1: *C. elegans* Strains used during genetic crosses

Strains in use were maintained by transferring two to four L4 hermaphrodites with the appropriate phenotype to a new plate twice a week and placed at 20 C. Strains not currently in use were maintained once a week and kept at 15 C. Plates which had starved were chunked and allowed to go through one to two generations before being used.

Genetic Crosses

Marker strains

Two strains were constructed so as to contain a gene for high incidence of male (him-5) and either a neural cell marker or an excretory cell marker. The neural cell marker, *flp-20::GFP*, labels ALM, AVM and PVM cells under UV light and the excretory cell marker, *pgp-12::GFP* , does the same for the excretory cell (figure 4). Although the initial strain is a *him-5* strain with an excretory marker (*bgIs312*), *pgp-12*::GFP was the desired marker in order to compare data with Stringham lab (Schmidt et al., 2009)

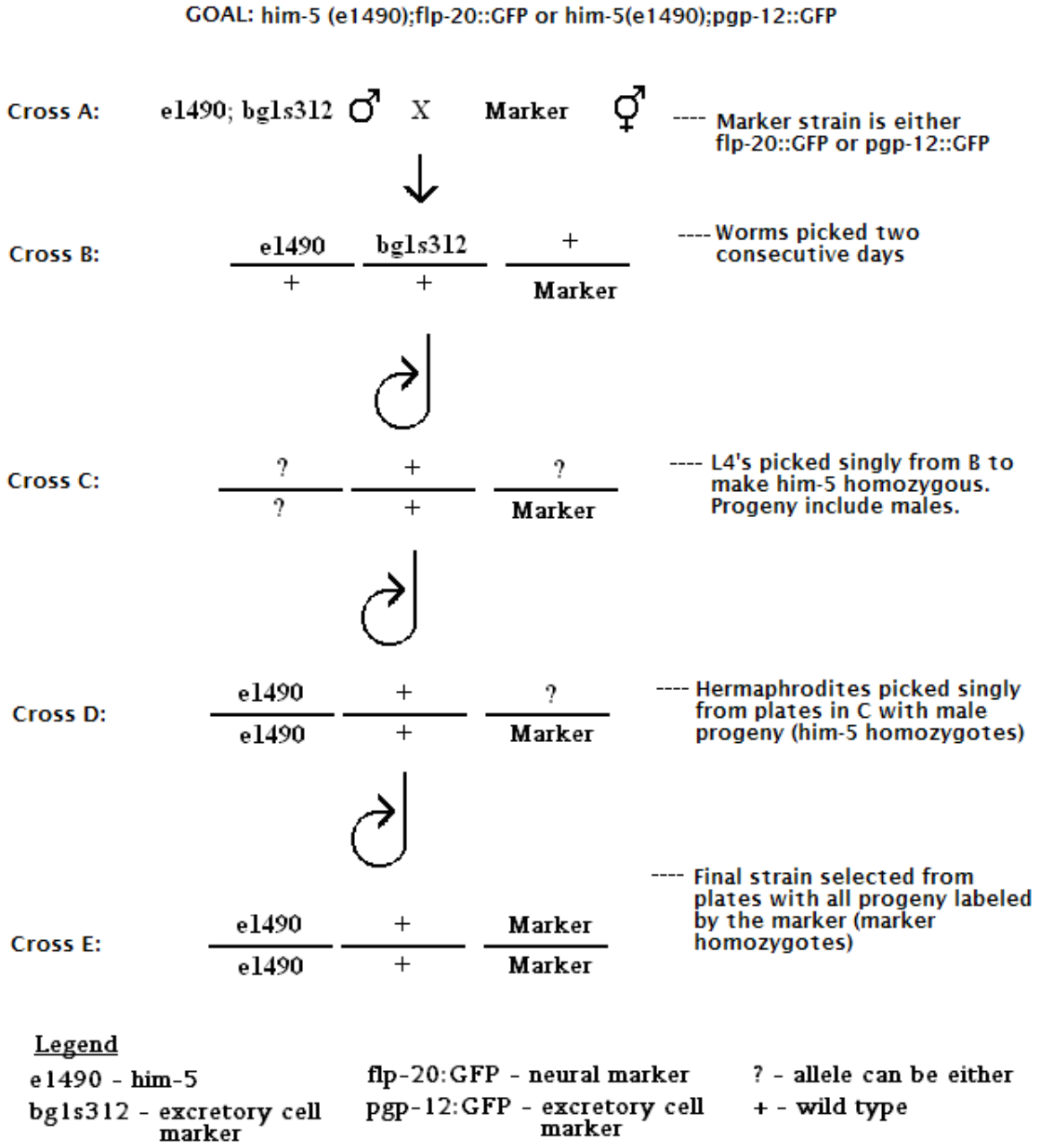

Figure 4: Strategy for creating Marker strains. Circling arrow, self cross

abi-1; flp-20:GFP

An *abi-1;flp-20*::GFP strain was constructed using the *him-5;flp-20*::GFP strain and VA74 (*abi-1;pgp-12*::GFP) strain(figure 5). The balancer strain JK2739 (*lin-6(e1466) dpy-5(e61)* I/hT2[qIs48] (I;III)) labels the pharynx due to the presence of the GFP transgene *qIS48*.

This strain was used to follow the presence of *abi-1* as the *abi-1(tm494)* does not cause an obvious plate phenotype. Four independent strains of *abi-1;flp-20::GFP* were observed.

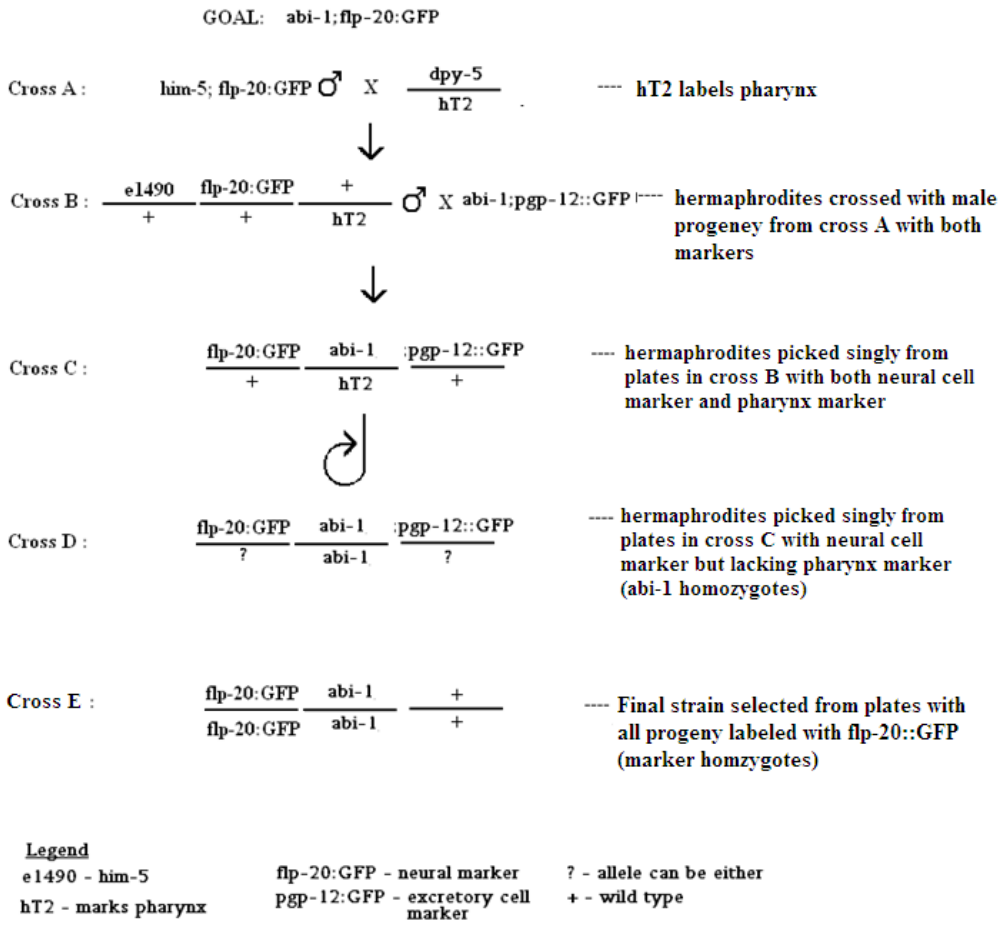

Figure 5: Strategy for creating *abi-1;flp-20*::GFP. Circling arrow, self cross

dpy-5;lin-53;flp-20::GFP and dpy-5;lin-53;pgp-12::GFP

lin-53;flp-20::GFP and *lin-53;pgp-12*::GFP constructs were made from MT8840 (*dpy-5*(e61) *lin-53*(n833) I) and either the *him-5;flp-20*::GFP or *him-5;pgp-12*::GFP strains (figure 6). *lin-53* was followed by the presence of a dumpy phenotype as *lin-53* and *dpy-5* are tightly linked. Dumpy worms are shorter and fatter then wild type worms and do not move as easily. During creation of the strains it was determined that *flp-20*::GFP was linked to *dpy-5 lin-53.* Because of

this, the final *dpy-5 lin-53 flp-20*::GFP strain was a recombinant product. Strains were confirmed by sequencing PCR products.

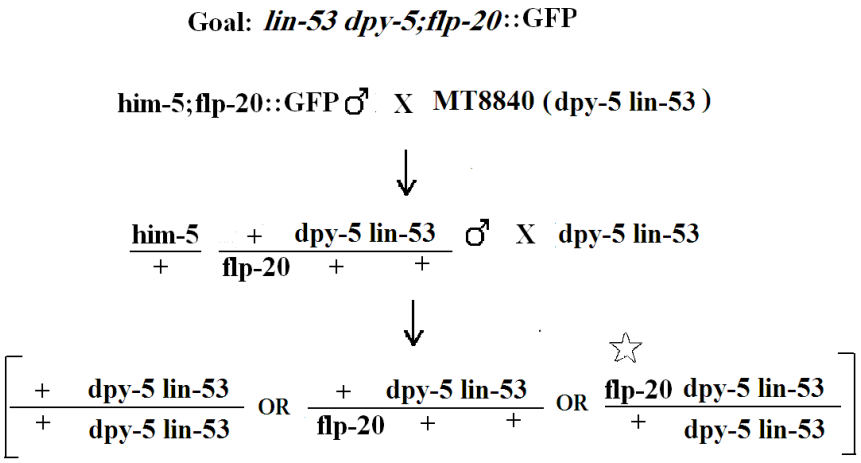

Figure 6: Strategy for creating *dpy-5 lin-53 flp-20*::GFP strain. The final recombinant product was the desired strain. ☆, recombinant product. (Legend same as figures 4 and 5).

mig-10; unc-53;pgp-12:GFP Double mutant

mig-10;unc-53;flp-20::GFP and *mig-10;unc-53;pgp-12*::GFP constructs were made from a *mig-10* strain, *unc-53* strain, *unc-53* balancer strain and either *him-5;flp-20*::GFP or *him-5;pgp-12*::GFP. (Figure 7). *unc-53* was followed using the balancer, *mIn1* (dpy)/*unc53; pgp-12*::GFP, which causes the pharynx to fluoresce green. Balancers suppress recombination and can be used to maintain lethal or sterile mutations in a heterozygous state. While it was unknown if the *mig-10;unc-53* doubles would be lethal, the balancer was used as it was unknown if an *unc-53* mutant would have an obvious phenotypic response in the targeted cells. Strains were confirmed by sequencing PCR products.

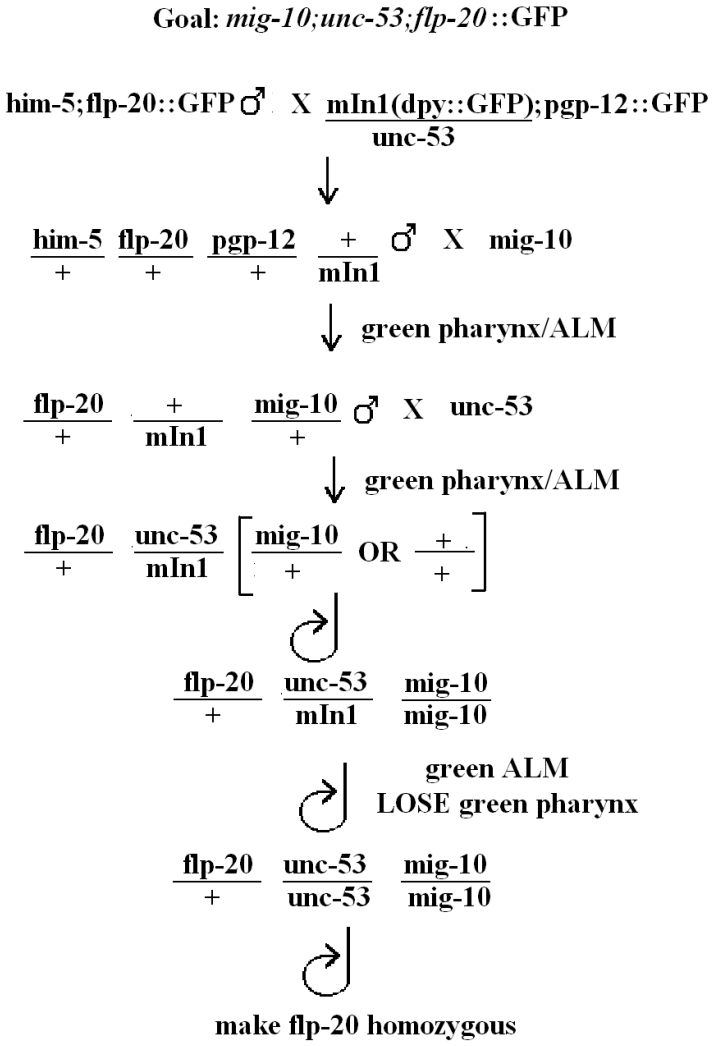

Figure 7: Strategy for creating *mig-10;unc-53;flp-20*::GFP Same strategy used for creating *mig-10;unc-53;pgp-12*::GFP. Legend same as figures 4and 5.

PCR Confirmation

The phenotypes of the *lin-53* and *unc*-53 genes was unknown prior to this project so the presence of the gene within the strain was confirmed genetically. Neither mutation changed the restriction enzymes recognizing the DNA sequence so Polymerase Chain Reaction (PCR) was used to determine the presence of the gene. PCR products were sent for sequencing. When needed, QiaQuick's gel purification system was used to purify PCR products before sending off for sequencing.

10 Worm PCR

2.5 µL of lysis buffer and enzyme solution (50 mM KCl, 10 mM Tris, pH 8.2, 2.5 mM $MgCl_2$, 0.45% NP-40, 0.45% Tween 20, 0.01% gelatin, 0.15 mg/mL Proteinase K (lysis enzyme)) was pipetted into the caps of PCR tubes. Approximately 10-15 worms were transferred into each tube cap. The tubes were quickly microcentrifuged then 50 µL of mineral oil was pipetted over the solution. The tubes were transferred into a -80ºC freezer for at least 30 minutes. The tubes were then placed into the thermocycler and the following lysis program was run:

1 hour @ 65ºC (lysis step)
15 min @ 95ºC (inactivation of Proteinase K)
Hold @ 4º C indefinitely

After the lysis step was completed, 22.5 µL of the master mix (14.9 µL rdH2O,2.5 µL 10X Long PCR Buffer 3 (Roche; contains $MgCl_2$), 0.6 µL 10 mM dNTP mix, 2 µL 5 µM forward Primer, 2 µL 5 µM reverse Primer, 0.5 µL Taq polymerase (Fisher Scientific)) was pipetted under the mineral oil of each tube. The tubes were returned to the thermal cycler and the following programmed cycle was run:

10 min @ 94º C (initial denaturing step)
Cycle 30 X:
    30 sec @ 94ºC (denature)
    1 min @ 60ºC (anneal)
    2 min @ 72ºC (primer extension)
10 min @ 72ºC (final extension)
Hold @ 4º C indefinitely

PCR Primers

Primers were used for PCR sequencing of the *lin-53* and *mig-10;unc-53* strains. The primers were designed to be approximately 22 bases in length with 50-60% G+C composition. The 3' ends of the primers were designed to have 3 of the last 5 bases a G or C.

Four primers were used for *mig-10* sequence (appendix A) these were:

WT1 (forward) – 5' TGTTTGAATTTTCAGAATCCGC 3'
WT2 (reverse) – 5' GGTTGGATTGTGAGAAGAAACA 3'
WT3 (Forward) – 5' AACRCAACRCRAGTAATGGTGG 3'

WT4 (Reverse) – 5’ GGATTCTTTGTGTACATTTGTGC 3’

Two primers were used for the *unc-53* sequence (appendix B) these were:

Forward – 5’ CTCGTTCAATGATCCTTCTCG 3’
Reverse – 5’ CGTGACTTGGAGTGTTACAAG 3’
Two primers were used for the *lin-53* sequence (appendix C) these were:

Forward -5’ TGTCTTCTGACACACTGCACAC 3’
Reverse – 5’ GTTGAAGATGTTGCTTGGCACG 3’

PCR analysis
The PCR reaction was confirmed by running the samples on a 1% agarose gel with 5 µL of 5 mg/ml Ethidium Bromide/100 ml of agarose. 5µL of Bromophenol Blue/glycerol solution was used as a marker in each sample. Gels were run at ~ 100amps for ~100 mins then samples were purified using Qiagen’s Qiaquick Gel extraction kit. The purified samples were sent to the DNA Analysis Facility on Science Hill at Yale University for sequencing.

ALM Migration Assay

To observe the ALM in the living animals they were washed from plates with M9 and then pipetted onto slides with a pad of agarose containing 20 µL of 1M azide/ 2 ml of 2% agarose. The azide stopped the animal’s movements without killing them, allowing the position of both ALM cell bodies to be observed in individuals. Initially, cell migration was inferred through position of the ALM in relation to the AVM. Wild type worms with normal cell migration have both ALM cell bodies posterior to the AVM. Subsequent quantifications were done via the IPLab software which allowed the distance from the vulva to the desired cell to be calculated in pixels.

Statistical Analysis

Two methods of statistical analysis were used to determine the significance of the data. The chi-square test was used to test the null hypothesis that there was no difference in the number of ALM neurons migrating to a particular region for *abi-1, mig-10*, and wild type strains. The

overall α value of 0.05 was divided by 3 to adjust for the 3 comparisons that were made (Bonferroni correction). The t-test was used to test the null hypothesis that the mean distance of ALM and AVM from the vulva was the same for various strains. Again, the α value was adjusted appropriately to compensate for multiple comparisons.

Results

Genetic mutants were constructed in order to observe *in vivo* effects of certain mutations on cell migration

In order to observe the *in vivo* effects of ABI-1, LIN-53 and UNC-53, it was necessary to have mutants with fluorescent markers for the excretory canal and migratory neurons. To create these desired strains, marker strains were created which had a high incidence of males (*him-5*) and either a neural cell marker (*flp-20*::GFP) or an excretory cell marker (*pgp-12*::GFP) (See Methods). Males from these him strains were crossed into *abi-1*, *lin-53*, *unc-53* and *mig-10* strains to create *abi-1;flp-20*::GFP, *lin-53;flp-20*::GFP and *mig-10;unc-53*;*flp-20*::GFP strains in order to observe the effects of the respective mutations on neuronal cell migration, specifically that of the ALM. Migration of the excretory canal was also of interest in the *lin-53* mutant so *lin-53;pgp-12*::GFP was created. Strains were sequenced to confirm identity, and it was discovered that the *mig-10;unc-53;flp-20*::GFP double mutant was not correct. Correct strains were then analyzed to determine the effect of each mutation on cell migration.

Abi-1 shows an effect on neuronal cell migration

Once mutant strains were created, the *in vivo* effects on cell migration were observed. The first strain measured was the *abi-1* mutant strain. Quantification of cell migration in the worm was measured by dividing the animal into three regions relative to the AVM. An ALM cell was identified as being in Region 1 if the cell body was anterior to the AVM, Region 2 if the cell body overlapped in the A-P dimension the AVM or Region 3 if it was posterior to the AVM (Figure 8).

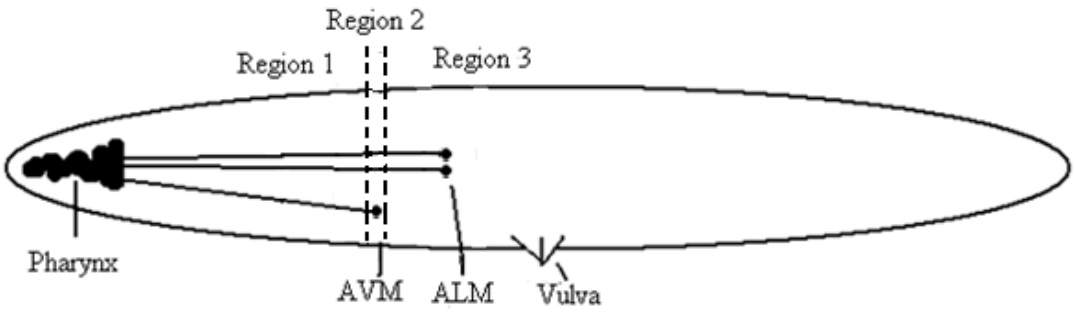

Figure 8: Schematic of wild type worm showing ALM quantification regions. Anterior is to the left. Region 1- Anterior to AVM; Region 2 – Equal with AVM; Region 3 – Posterior to AVM.

Migration of the ALM is from anterior to posterior, with the ALM in wild type animals migrating past the final position of the AVM neurons (figure 9A and 9B). *abi-1* and *mig-10* mutant animals showed similar phenotypes (Figure 9C and 9D, Figure 10) with the ALM often migrating to a position anterior of or equal to the AVM. All strains had some variability, however *abi-1* and *mig-10* mutants showed this phenotype to a much greater extent than wild type.

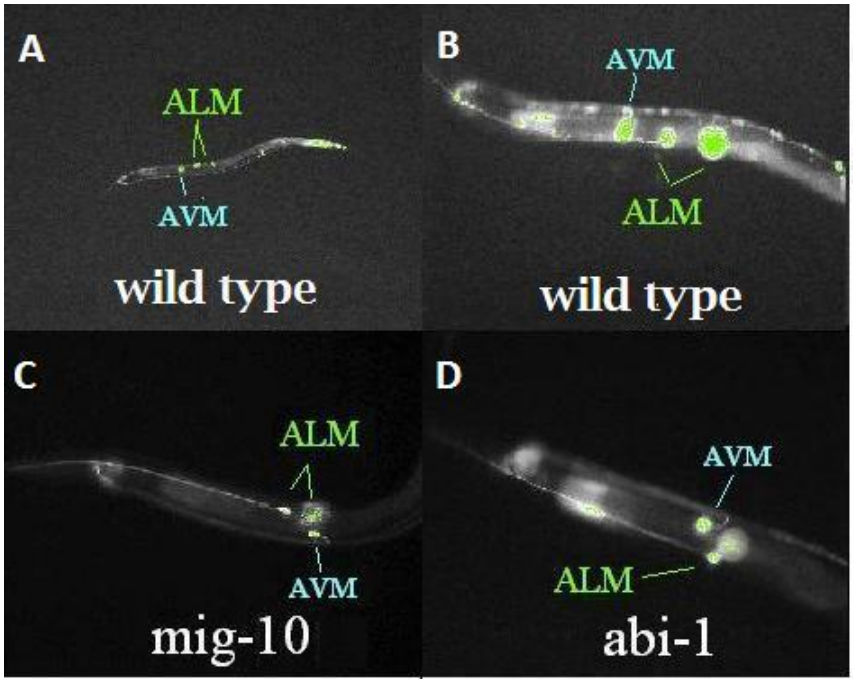

Figure 9: ALM cell migration in *abi-1, mig-10* and wild type animals. A and B) *him-5;flp-20*::GFP, B is higher magnification. C) *mig-10;flp-20*::GFP. D) *abi-1:flp-20*::GFP Anterior is to left.

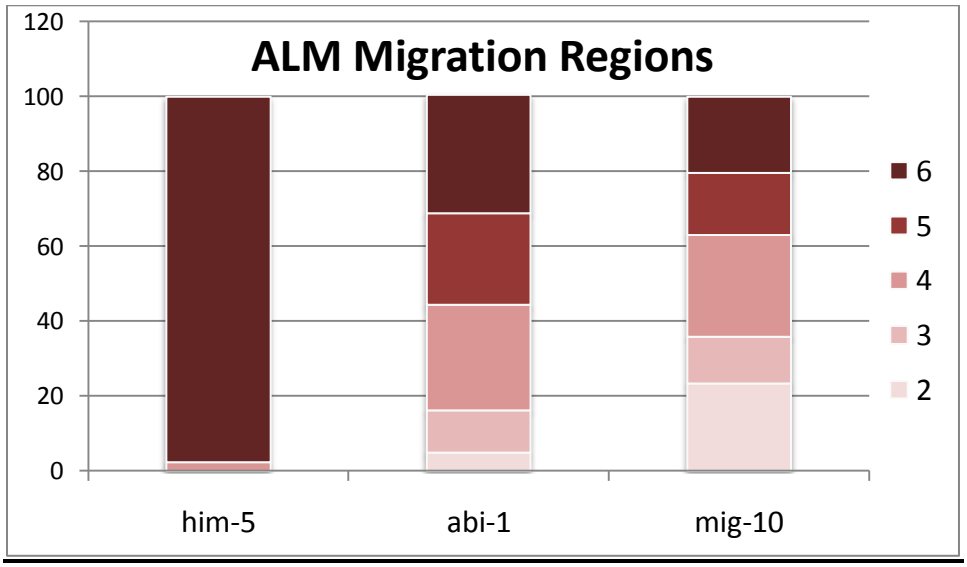

Figure 10: Region comparison between wild type, *abi-1* and *mig-10*. The scores for the two ALM cell bodies were added together for each animal, resulting in each animal having a score between 2 and 6. Wild type (*him-5*) N = 44; *abi-1* N=114; *mig-10* N=103.

The migration defect was quantitated by region for each strain (Figure 10). The most evident result in figure 10 is the marked difference between the wild type strain and either mutation. A chi-square test was performed to determine statistical significance. Using a conservative α-value of 0.016 to adjust for multiple comparisons, it was determined that both *abi-1* and *mig-10* were significantly different from the *him-5* strain. The *abi-1* and *mig-10* strains appear to be similar, however a chi-square test performed determined that *abi-1* was significantly less severe than *mig-10.* While this difference is interesting to note, it is not truly meaningful as the *abi-1* allele used is not predicted to completely inactivate the protein. (Schmidt et al, 2009) A null mutation, would likely show more severe effects than the weak allele that was used.

A *lin-53;dpy-5* mutant perturbs neuronal migration

In order to more accurately quantify cell migration in the *lin-53;dpy-5;flp-20*::GFP and *mig-10;unc-53;flp-20*::GFP strains a different method was used for the remaining quantifications. In the newer method, the distance was measured from the vulva to each cell body by taking a picture of the animal and using the CamWare IP LAB software, which allowed the distance to be counted in pixels. The data was normalized by the length of the vulva to the pharynx to account for the size of the worm. Unlike the regional quantification, measuring cell position with respect to the vulva allowed us to distinguish effects of various mutations on ALM migration from effects on AVM migration.

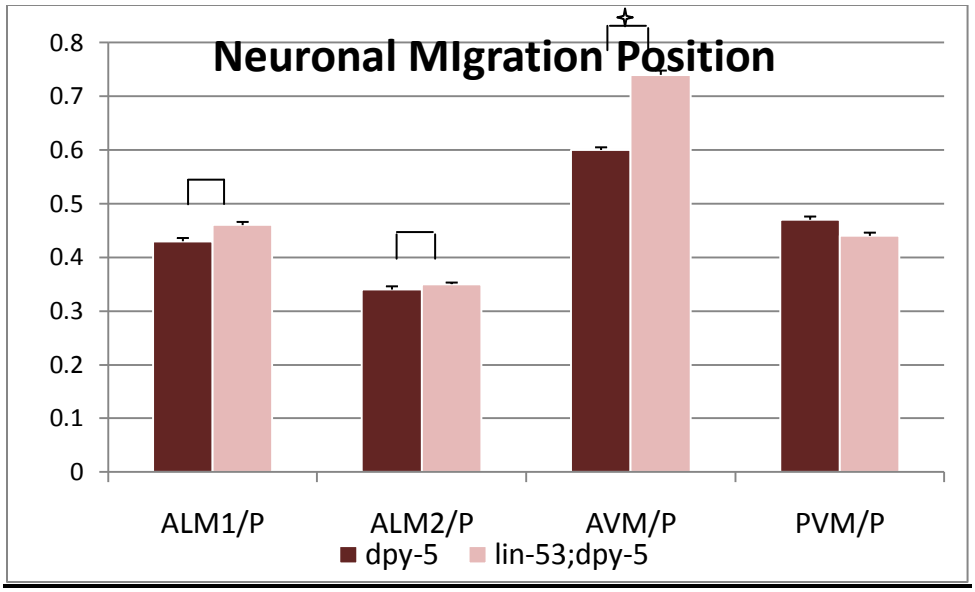

Figure 11: Cell body Distance in *dpy-5* and *dpy-5 lin-53* mutants. Distance from the vulva to each cell body was measured in pixels and normalized with the distance from the pharynx to the vulva. The two ALM cell bodies were distinguished by the distance of their migration with the cell migrating the shortest distance denoted as ALM1. Bars represent the standard error for each data set. *dpy-5* N=15; *dpy-5 lin-53* N=15. ⊤, statistical test performed. ✧ , p = .0004

A *dpy*-5 strain was used to compare to *dpy-5 lin-53* cell migration as this was the genetic background of the strain. *Dpy* animals are shorter and fatter than wild type animals. There appear to be minimal differences between the ALM migration of the *dpy* control and the *lin-53;dpy* worm, however these differences are not significant (Figure 11). The AVM appears to differ greatly, however, and this difference was shown through a t-test to be statistically significant (p=.0004). These data indicate that *lin-53* appears to increase the length of AVM migration, unlike *mig-10* which truncates migration of both ALM and AVM (Figure 12).

An *unc-53* mutant affects AVM migration in the opposite direction as *mig-10*.

The same method for quantifying cell body migration in the *lin-53* mutant was used to quantify an *unc-53;flp-20*::GFP mutant. The data shows a significant difference between the wild type and *mig-10* animals not only for ALM migration, but also AVM migration (p=.006) (figure

12). *unc-53* also showed a difference in AVM migration from wild type animals, however the difference was not significant for the small population studied. *unc*-53 did not affect ALM migration. Interestingly, *unc-53* and *migh-10* affect AVM migration in different directions and thus are highly significant from each other.

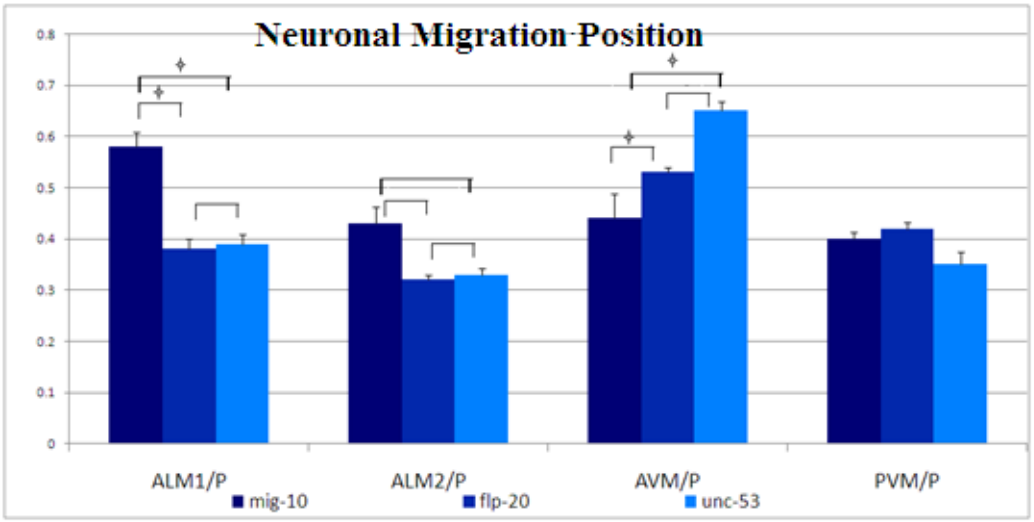

Figure 12: Cell body distance in wild type, *mig-10* and *unc-53* mutants. Distance from the vulva to each cell body was measured in pixels and normalized with the distance from the pharynx to the vulva. Bars represent the standard error for each data set. *mig-10* data collected by Elizabeth Ryder. N= ~15 for each strain. .| |, statistical test performed. ✦ , p < .006

While attempting to create the *mig-10;unc-53;flp-20*::GFP mutant strain, one interesting phenotype was observed which was also present in the *unc-53;flp-20*::GFP single mutant.(Figure 13). In wild type animals, the PVM precursor cell originates from the same position as the AVM precursor cell and migrates posteriorly, whereas the AVM migrates anteriorly. This results in the PVM migrating to a position in the posterior half of the animal. In a small number of animals in both the *unc-53* single mutant strain, and in animals thought to be *mig-10;unc-53;flp*-20::GFP, the PVM migrated anteriorly, resulting in a position close to (Figure 13) or even anterior to the vulva.

Figure 13: Abnormal PVM migration in putative *mig-10;unc-53;flp-20*::GFP animal. Combined fluorescent- Nomarski photograph of L4 double mutant. AVM, both ALM cell bodies and PVM pictured. Anterior to the left.

Discussion

Candidate genes are relevant *in vivo*

One of the main goals of this project was to determine if the genes identified during the previous project's yeast two hybrid screen were relevant *in vivo*. The project looked at effects of *abi-1*, *lin-53*, m*ig-10* and *unc*-53 mutations on the migration of the ALM and AVM. During embryogenesis the ALM migrates anterior to posterior, while the AVM migrates posterior to anterior during L1. The results of this project do show that *abi-1* and *lin-53* are both relevant *in vivo* and that mutations within these genes cause abnormal cell migration.

It is fairly evident from this work that a mutation in *abi-1* affects ALM final position with respect to AVM similarly to the effects of a *mig-10* mutation. This can be seen not only through its marked difference with the wild type phenotype, but also its significant similarities with *mig-10*. Both the *abi-1* and *mig-10* animals showed ALM positions much more anterior to the AVM than wild type. The *abi-1* mutation used was not a null and it would be interesting to see the severity of the mutant phenotype with a null mutation. There are a few problems with using a null mutation for *abi-1*, the first being that there are no available alleles with null mutations. More importantly, it is not known if a strain carrying null mutation would be viable as ABI-1 is required for embryonic development and a full knockout of gene function may be lethal.

Prior to this work, it was thought that a mutation in *mig-10* only affected migration of the ALM and not the AVM. Through data collected during this project, it was discovered that the *mig-10* mutation decreases anterior migration of the AVM. This results in an AVM which is in a more posterior position than normal. Since the quantification method used to evaluate the position of ALM in *abi-1* was relative to the AVM, it is unknown whether *abi-1* is primarily affecting ALM or AVM migration, or both. Future work should address this question.

Though the second candidate *lin-53* did not appear to affect ALM migration, it did significantly increase AVM migration. This was a new and unexpected phenotype, since it is opposite to that of *mig-10* mutations; however it does show that *lin-53* plays a role in cell migration. *mig-10* is involved in migration of both the AVM and ALM (this work). . *lin-53*'s

effect on AVM migration supports the idea that MIG-10 interacts with different partner proteins to perform different types of migrations, since *lin-53* interacts with *mig-10* but only affects AVM migration.

The fact that ABI-1 and LIN-53 do appear to play a role in migration *in vivo* supports the idea that they may be in a pathway with MIG-10, as suggested by the yeast two hybrid screen. Since it has been shown that mutations in *abi*-1 and *lin-53* do affect cell migration *in vivo*, further studies should create double mutants for both with *mig-10*. Though a *abi-1 mig-10* double mutant would be difficult to make as the genes are tightly linked, the double mutant would confirm that the candidate is in the same genetic pathway as *mig-10* if it produces a phenotype which does not enhance the *mig-10* migration mutations.

This work shows that *mig-10* and *lin-53* are both required for normal AVM migration, however their mutations cause abnormal migration in different directions. There are two possible types of interactions between MIG-10 and LIN-53 which would account for this directional difference: the two proteins may be in the same or independent pathways that affect AVM migration. Determining the phenotype of the double mutant would help in determining the relationship of *mig-10* and *lin-53*. As this is a signaling pathway, if one is upstream of the other in the same signaling pathway, the double mutant should show the phenotype of the downstream mutation. As LIN-53 is a nucleosome remodeling factor and MIG-10 is located in the cytoplasm, *lin-53* would be the epistatic gene and the double mutant would show the *lin-53* mutant phenotype. If the two are working independently, then the two would suppress each other and the double mutant would show a phenotype more similar to the wild type phenotype.

Unc-53 appears to influence both AVM and PVM migration

The second goal of the project was to determine if *unc-53* was in the same genetic pathway as *mig-10*. Unfortunately that conclusion cannot be made by this project as the *mig-10;unc-53* double mutant was not confirmed. Further studies should continue with the double mutant, both in constructing the strain and performing quantification of cell migration.

There was one unique result concerning the putative double mutant strain used during this project. Though sequencing showed that the strain used did not contain the *mig-10* mutation, there was an abnormal PVM migration phenotype present within the strain, in which the PVM migrated posterior to anterior instead of anterior to posterior. This phenotype was also noted in the single *unc-53* mutant, however to a lesser degree than the putative 'double' mutant strain. This increase in prevalence may indicate that the strain was initially heterozygous for *mig-10*, and some animals may have been *mig-10* homozygotes.. If this was the case, a correct double should show an enhancement of the *unc*-53 mutant PVM phenotype.

Though the *mig-10;unc-53;flp-20*::GFP double mutant was unable to be studied during the course of this work, it was shown that *unc-53* affects AVM but not ALM migration. Though the differences in AVM migration were not significant for the sample size used, *unc-53* showed AVM migration similar to *lin-53*, which was in the opposite direction of the *mig-10* effects. To truly determine the significance of the *unc-53* effects, the study should be replicated with a larger sample size. If a significant difference in AVM migration between wild type and *unc-53* animals is observed, similar conclusions can be drawn between the interaction of *unc-53* and *mig-10* as were made for *mig-10* and *lin-53*. It has been suggested that *unc-53* may act as a scaffold to link extracellular cues to the intracellular cytoskeleton (Strigham et al, 2009), so if they are in the same pathway, *unc-53* would be upstream and the double mutant would show the *mig-10* mutant phenotype.

This project showed that the proteins identified by the yeast two hybrid study previously performed are not only relevant *in vivo*, but that *mig-10* is involved in different pathways to perform different types of migration. One of the most interesting conclusions regards *lin-53* and *unc-53* mutants directing AVM migration in the opposite direction as *mig-10* mutants. Future research should look more closely at these effects in order to better understand the complex interactions *mig-10* is involved in while performing the different types of migrations.

Citations

Brenner, S. (May 1974). The Genetics of *Caenorhabditis elegans*. *Genetics* **77**: 71–94. Chang, C., Adler, C. E., Krause, M., Clark, S. G., Gertler, F. B., Tessier-Lavigne, M., Bargmann, C. I.. (2006). MIG-10/Lamellipodin and AGE-1/PI3K Promote Axon Guidance and Outgrowth in Response to Slit and Netrin**.** *Current Biology* **16**, 854-862

Disanza, A., Steffen, M., Hertzog, E., Rottner, K., Scita, G. (2005). Actin polymerization machinery: the finish line of signaling networks, the starting point of cellular movement. Cellular and Molecular Life Sciences **62**, 955-970

Ficociello, L and Ryder, E. (2007) *Neuronal Migration: Investigating MIG-10 interaction with Ras GTPases in C. elegans.* International Worm Meeting.

Hekimi, S. and Kershaw, D. (1993) Axonal guidance defects in a Caenorhabditis elegans mutant reveal cell-extrinsic determinants of neuronal morphology. *Journal of Neuroscience*. 13(10): 4254-4271

Lafuente, E., van Puijenbroek, A., Krause, M., Carman, C., Freeman, G., Berezovskaya, A., Constantine, E., Springer, T., Gertler, F. and Boussiotis, V. (2004).RIAM, an Ena/VASP and Profilin ligand, interacts with Rap1-GTP and mediates Rap1-induced adhesion. *Developmental Cell*. 7(4):585-95.

Legg, J. and Machesky, L. (2004) MRL proteins: Leading Ena/VASP to Ras GTPases. *Nature Cell Biology*. **6**: 1015-1017.

Manser, J., Rooprapunt, C., Margolis, B., *C. elegans* Cell Migration Gene*mig-10*Shares Similarities with a Family of SH2 Domain Proteins and Acts Cell Nonautonomously in Excretory Canal Development (1997) *Developmental Biology* **184**, 150-164

Manser, J. and Wood, B. (1990). Mutations Affecting Embryonic Cell Migrations in Caenorhabditis elegans. *Developmental Genetics*. **11**, 49-64

O'Toole, S. and Gosselin, J. (April 2008). MIG-10, an Adapter Protein, Interacts with ABI-1, a Component of Actin Polymerization Machinery. WPI MQP.

Quinn, C. C., Pfeil, S. D., Chen, E., Stovall, L. E., Harden, V. M., Gavin, K. M., Forrester, C. W., Ryder, F. E., Soto, C. M. and Wadsworth, G. W. (2006) UNC-6/Netrin and SLT-1/Slit Guidance Cues Orient Axon Outgrowth Mediated by MIG-10/RIAM/Lamellipodin. *Current Biology*. **16**, 845-853.

Quinn C.C. and Wadsworth W.G. (2008). Axon Guidance: Asymmetric Signaling Orients Polarized Outgrowth. Submitted for publication.

Schmidt, K., Marcus-Gueret, N., Adeleye, A., Webber, J., Baillie, D. and Stringham, E. (2009) The cell migration molecule UNC-53/NAV2 is linked to the APR2/3 complex by ABI-1. *Development.* **136**(4): 563-574.

Strigham, E., Pujol, N., Vandekerckhove, J. and Bogaert, T. (2002) unc-53 controls longitudinal migration in C. elegans. *Development*. **129** (14): 3367-3379.

Vicente-Manzanares,M., Webb, D., & Horwitz, A. (2005) Cell Migration at a glance. Journal of Cell Science. **118**: 4917-4919.

Wormatlas.org

Wormbase.org

Xiaowei, Lu; Horvitz, Robert. "*lin-35* and *lin-53*, Two Genes that Antagonize a *C. elegans* Ras Pathway, Encode Proteins Similar to Rb and Its Binding Protein RbAp48." (1998)Cell **95**, 981–991

Appendices

Appendix A: mig-10 Sequence and primers

total length 899

ct41 mutation shown in green. WT=c, mig-10(ct41)=t (Gln → stop)

mutation at 439 (460 from 3' end)

primers: WT1 (F) and WT2 (R) in pink; WT3 (F) and WT4 (R) in cyan

WT PCR Product

```
TATGAACAAT TTTAATATAA TAATTATTAT ATTCAAAGAG TATTATCCTA
TGATAATAAT TGTTTGAATT TTCAGAATCC GCAGATTGGC AGTTGGATGA
ACTTCTTGAA GAATTGGAAG CTCTTGAAAC TCAACTCAAC TCTAGTAATG
GTGGAGATCA ACTTTTACTT GGTAATTTTT ATGTTTTGGA ATTTTTTTGA
ACTTCCAACA ATTTTATTTA ATTTAAAAAA TGTGAAACAC CAGAAAACCT
ACGAGATGGC AATTTTTACA AAATTTCAAA CTCTAAATTT TTCAGGAGTG
TCCGGGATTC CAGCTTCTTC TAGCCGGGAA AATGTGAAGT CAATATCCAC
ACTGCCACCT CCACCACCGG CTCTTTCTTA TCACCAAACT CCACAACAAC
CTCAACTTTT ACATCATCAC AATAATCATT TGGGTTATCA GAATGGTATT
CATCAGGTTT GTGATTTTTT GTTGAAAATT TTGAAAAAAT AGTATAAGTG
ATATATAACG TTTCCTAGTT TTGAAATTTT GGCATCTATT TTTTCAAATT
TTAAAGAATG CTCATAACCA TAGAAAATGA ATTCTTCCAA TTTGTTTATA
CTTGAATCAA CATCCTGTTC TTCTGTTCCA CTGAACAGCA GACCTCAGCC
CCATCTTTGT ATAAAGTGAA TACGAACGCC TTTTGCTCAC AATCCCCCTC
TCCTTTTGCA CAAGAAATTT GATTTGTCTT CTGTGGCGAG ACTCTGCTTT
CCTTCCTGAG CTCCAACTGG TTGCTCTCTC TCTCTTTCTC GAAATTTGAT
ACAAGTCGTC ATGATGCTCT CTGATGATGT TGATGATCAT GTACAAGAGA
GGATTCTTTG TGTACATTTG TGCATATGGT TGGATTGTGA GAAGAAACA
```

ct41 mutant PCR product

```
TATGAACAAT TTTAATATAA TAATTATTAT ATTCAAAGAG TATTATCCTA
TGATAATAAT TGTTTGAATT TTCAGAATCC GCAGATTGGC AGTTGGATGA
ACTTCTTGAA GAATTGGAAG CTCTTGAAAC TCAACTCAAC TCTAGTAATG
GTGGAGATCA ACTTTTACTT GGTAATTTTT ATGTTTTGGA ATTTTTTTGA
ACTTCCAACA ATTTTATTTA ATTTAAAAAA TGTGAAACAC CAGAAAACCT
```

ACGAGATGGC AATTTTTACA AAATTTCAAA CTCTAAATTT TTCAGGAGTG
TCCGGGATTC CAGCTTCTTC TAGCCGGGAA AATGTGAAGT CAATATCCAC
ACTGCCACCT CCACCACCGG CTCTTTCTTA TCACCAAACT CCACAACAAC
CTCAACTTTT ACATCATCAC AATAATCATT TGGGTTATTA GAATGGTATT
CATCAGGTTT GTGATTTTTT GTTGAAAATT TTGAAAAAAT AGTATAAGTG
ATATATAACG TTTCCTAGTT TTGAAATTTT GGCATCTATT TTTTCAAATT
TTAAAGAATG CTCATAACCA TAGAAAATGA ATTCTTCCAA TTTGTTTATA
CTTGAATCAA CATCCTGTTC TTCTGTTCCA CTGAACAGCA GACCTCAGCC
CCATCTTTGT ATAAAGTGAA TACGAACGCC TTTTGCTCAC AATCCCCCTC
TCCTTTTGCA CAAGAAATTT GATTTGTCTT CTGTGGCGAG ACTCTGCTTT
CCTTCCTGAG CTCCAACTGG TTGCTCTCTC TCTCTTTCTC GAAATTTGAT
ACAAGTCGTC ATGATGCTCT CTGATGATGT TGATGATCAT GTACAAGAGA
GGATTCTTTG TGTACATTTG TGCATATGGT TGGATTGTGA GAAGAAACA

Appendix B: *Unc-53* sequence and primers

N152 in exons 18, 19 and interons between 18/19 and 19/20. Takes out all of 19 and ~90 bp of 18 (marked off by | |)

N166 in Exon 20 marked by green
Final primers in cyan

n166 in green (C -→ T in mutant; makes CAA → UAA therefore Q → stop

```
   CAFCCGC CCTCAACGCT TCGGGTATGT CTCGTTCAAT GATCCTTCTC
GAATCCCTTT CACCACGACC ACCTCGACGT CACCAATCAC CGGCTGACTC
GTGCATTATC ACAGCTTCTC CATCAGCCCC ACGAAGATCA CATTCGCCAC
GTGGCCCCAC CGCCCGTATC CCACTTTCTC TCGCTTCTTC GCCTGTCCAC
GTCAATAACA ATTGGGGATC CTACTCGGCG CGTTCCCGAG GTGGAAGCTC
TACTGGTATC TATGGAGAGA CGTTCCAACT GCACAGACTA TCCGATGAAA
AATCCCCCGC ACATTCTGCC AAAAGTGAGA TGGGATCCCA ACTATCACTG
GCTAGCACGA CAGCATATGG ATCTCTCAAT GAGAAGTACG AACATGCTAT
TCGGGACATG GCACGTGACT TGGAGTGTTA CAAGAACACT GTCGACTCAC
TAACCAAGAA ACAGGAGAAC TATGGAGCAT TGTTTGATCT TTTTGAGCAA
AAGCTTAGAA AACTCACTCA ACACATTGAT CGATCCAACA TGAAGCCTGA
AGAGGCAATA CGATTCAGGC AGGACATTGC TCATTTGAGG GATATTAGCA
ATCATCTTGC ATCCAACTCA GCTCATGCTA AC
```

Forward
CTCGTTCAATGATCCTTCTCG

Reverse
CGTGACTTGGAGTGTTACAAG
GCACTGAACCTCACAATGTTC comp
CTTGTAACACTCCAAGTCACG reverse comp = primer

Appendix C*: Lin-53* sequence and primers

N833- top strand 5'->3'
mutation in green (bp 451, A -> T)
primers in cyan

```
AAAACTTAGT TGGTGAAGAA TATGCGTTTG AATAAATGGT AAGATGAACA
ATTTGTTGAG ATGCAAAATT AAAGAAGGAT AGAAGTTAAA TACAAATAAT
TTAAGCGCGT TTCACGTATT TTACTGTTGT CTCTCTACCA CATCGGCTGG
AGTTTCTTCG TCAACTTCGT TGTATATGTT ATCAGCCATT TGCCACACTT
GGAGAATATT GTCTTCTGAC ACACTGCACA CAACCCAAGG CTCGTTCGGG
TTCCACGAGA AATCGCTGAT CTTGGCGGTG TGCCCACCGT GAATAAACAA
CAGCTCTGGT GGACCATCTT CCGCGTCTTC GGCAGATTGG TCTTCTCCAA
TCTTAGATAG GTCCCACACA TGAAGACGTT TATCAGTACC GCTGGATGCA
AGAATAGTCT CGTTGTGTGG ACTCCACTGA ACTTGGAAGA TTTCATCACG
ATGTGATTCA AATGAGTGAA GTTTCATTCG TAGATTACGT AGATCCCAAA
AAGCGACAGT TTTATCAGCT GATCCGGTGG CCAGAATGAA TTCGGAATAT
GGATTGAATG CGAGACAGTT AACTTCGGCA GAATGAGCAT CGATACAGTG
TCCAGGAGTG CTTGTGCGCA CATCCCAAAT GAGCCTATAA TTTTTAATTA
GTTAATAAAT AGAAAAAAAA CAAAAGCTTA CAATTTTCTA TCGTCACCAA
CCGATCCGAA GACACCATCA TGCAAAACGT GCCAAGCAAC ATCTTCAACG
ACTGACTCGT GACCTTTGAA AACATCCTTC GCTTGCAATT CCCCGGCAAC
ATTCTGATTT GCGTTGATAT CCCAATGACA AACTGTCTGA TCATCTGACG
CTGATAGAAT CAAACCTTCT TTGTTTGGAT TCCATGATAA TCCATAGCCT
TCCTTCGTGT GTCCTTTCAG TCTGATAAGC GGATTGAACG TGTTATCACG
AGGAACAGCA GAGTGCTTTA AATAGTCGAA AATGTAAACA TCAGCATGTG G
```

Forward:

5' TGTCTTCTGACACACTGCACAC 3'

Reverse:

5' GTTGAAGATGTTGCTTGGCACG 3'